AIChE WILEY InterScience DISCOVER SOMETHING GREAT

SEPARATIONS

Composite Membrane Based on Ionic Conductor and Mixed Conductor for Oxygen Permeation

Xuefeng Zhu and Weishen Yang
State Key Laboratory of Catalysis, Dalian Institute of Chemical Physics, Chinese Academy of Sciences, Dalian 116023, China

DOI 10.1002/aic.11410
Published online January 24, 2008 in Wiley InterScience (www.interscience.wiley.com).

A composite membrane, which comprises of one fluorite oxide phase ($Ce_{0.8}Gd_{0.2}O_{1.9}$) for oxygen ionic transport and one perovskite oxide phase ($Gd_{0.2}Sr_{0.8}FeO_{3-\delta}$) for both oxygen ionic and electronic transport, was investigated. XRD results revealed that the two oxides are compatible and showed good oxygen permeation stability at 950°C (more than 1100 h). Oxygen flux of the composite membrane was two times higher than that of the $Gd_{0.2}Sr_{0.8}FeO_{3-\delta}$ mixed conducting membrane at the same conditions. At steady state, oxygen flux of a 0.5 mm membrane was 0.80 ml/(cm^2 min) under oxygen partial pressure gradient of air/He and ~5.0 ml/(cm^2 min) for syngas production at 950°C, respectively. After ~440 h operation under syngas conditions, SEM analysis revealed that the syngas side of the membrane still kept dense and the EDX showed the transfer of elements occurred in the depth of a few microns. © 2008 American Institute of Chemical Engineers *AIChE J,* 54: 665–672, 2008
Keywords: composite membrane, ceria, oxygen separation, ceramic membrane, syngas

Introduction

During the past two decades, mixed conducting perovskite oxides have been deeply investigated as dense ceramic membranes for oxygen separation and conversion of light hydrocarbons.[1–6] Of particular significance is the partial oxidation of methane to syngas gas (CO + H_2).[4–6]

$$CH_4 + \frac{1}{2}O_2 = CO + 2H_2 \quad \Delta H(298\,K) = -35.67\,kJ/mol \quad (1)$$

This is because of a 25% reduction in the current technology-based cost of gas-to-liquids (GTL) product.[7] Usually, the traditional oxygen permeable materials, such as La_{1-x}(Ba, Sr, Ca)$_x$Co$_{1-y}$(Mn, Fe, Ni, Cu)$_y$O$_{3-\delta}$ ($0 \le x \le 1$, $0 \le y \le 1$), contain reducible $Co^{3+/2+}$, thus these materials have poor stability under reducing environments at elevated temperatures and are not suitable to construct membrane reactors for long-term operation under syngas production conditions.[8,9] Partial or total substitution of reducible cobalt in the B-site with less reducible ions (such as Al^{3+}, Ga^{3+} Ti^{4+}, Zr^{4+}, Ce^{4+}, etc.) was employed to improve the stability of these perovskite oxides.[10–13] Although the stability under reducing environments was improved in a way, the phase decomposition under great oxygen partial pressure gradient could not be avoided.[10]

Dual-phase composite materials were suggested as candidates instead of single-phase mixed conducting materials for application as oxygen separation membranes, since it is difficult to meet all the requirements (such as high permeability, stability, mechanical strength, etc.) in a single-phase membrane material. Generally, the improvement in some aspects for a single-phase mixed conducting membrane is simultaneously degradation in other aspects. Therefore, dual-phase membranes with changeable phase compositions made from oxygen ionic conducting phase and electronic conducting phase are suggested as alternatives to avoid the dilemma.

Composite membranes made of noble metal and oxide ionic conductors were firstly used as oxygen separation

Correspondence concerning this article should be addressed to W. S. Yang at yangws@dicp.ac.cn.

membranes, such as Ag-Bi_2O_3, Pd-YSZ (yttria-stabilised zirconia), etc.[14–16] However, these materials still have some disadvantages. First, to achieve a continuous electron transport network in the bulk, the volume fraction of noble metal phase usually exceeds 30%, which leads to high costs. Secondly, noble metal phase obstructs the transport of oxide ions between the oxide ionic conductor grains, which leads to the decrease of oxygen ionic conductivity. Thirdly, the mismatch of thermal expansion coefficient between metallic phase and ceramic phase is going to break the membrane during thermal circles.

To overcome these disadvantages, perovskite oxides were proposed to replace noble metals for electron transport. Kharton et al.[17] reported a kind of ceria based composite membranes, which contain a perovskite phase of $La_{0.7}Sr_{0.3}MnO_3$ (LSM) for electrons transport and a fluorite phase of $Ce_{0.8}Gd_{0.2}O_{1.9}$ (GDC) for oxygen ion transport. However, the oxygen permeation flux of the composite membrane was very low (about 0.05 ml/(cm^2 min) at 950°C), and decreased with operation time. After 800 h operation, the oxygen permeation fluxes were one order lower than the initial value. They attributed the degradation to the formation of layers with low ionic conductivity at GDC grain boundaries by interdiffusion of phase components. Subsequent researches on $La_{0.8}Sr_{0.2}Fe_{0.8}Co_{0.2}O_3$-$(La_{0.9}Sr_{0.1})_{0.98}Ga_{0.8}Mg_{0.2}O_3$ also exhibited the similar interdiffusion of the components, which degraded the ionic conductivity.[18] Sirman and Chen[19] reported a series of composite membranes based on GDC and $La_{0.8}Sr_{0.2}Co_{0.2}$ $Fe_{0.8}O_{3-\delta}$ (LSCF) with different volume ratio of the two oxides. Nevertheless, the long-term operation stability was not included. Composites of $Ce_{0.8}Gd_{0.2}O_{1.9}$-$Gd_{0.7}Ca_{0.3}CoO_{3-\delta}$ were also investigated as oxygen permeable membranes for NO_x detection in exhaust gases. However, the decomposition of the perovskite phase and interdiffusion of metal ions resulted in a relatively poor ionic transport property of the composites.[20]

Although pure electronic conductors, such as La_{1-x}(Sr, Ca)$_x$$MnO_3$, La_{1-x}(Sr, Ca)$_x$$CrO_3$, etc., with high chemical stability were suggested to replace noble metal as electronic conducting phase,[17] the poor oxygen ionic conductivity of these oxides blocks the transport of oxygen ions between grains of fluorite phases. Therefore, here, the mixed conducting perovskite oxides for transport of both electrons and oxide ions are proposed instead of electron conducting perovskite oxides to improve the permeability of composite membranes.[19]

Here, we report a ceria based oxygen permeable membrane of 60 wt % $Ce_{0.8}Gd_{0.2}O_{1.9}$−40 wt % $Gd_{0.2}Sr_{0.8}FeO_{3-\delta}$ (abbreviated as GDC-GSF), which showed a good oxygen permeation stability (stable for more than 1100 h operation) and high oxygen permeation flux of 0.80 ml/(cm^2 min) at 950°C under an oxygen partial pressure gradient of 21 kPa/0.5 kPa. After 440 h syngas production experiment, the oxygen permeation flux increased to ~5.0 ml/(cm^2 min).

Experimental

Membrane preparation

The $Ce_{0.8}Gd_{0.2}O_{1.9}$ oxide (GDC) and $Gd_{0.2}Sr_{0.8}FeO_{3-\delta}$ oxide (GSF) were synthesized by the combined citric acid and EDTA process. Metal nitrates solution concentrations were determined by titration. The required amounts of the solutions were introduced into a beaker, and equal molar of citrate and EDTA respect to total metal ions were added. Then the pH value was adjusted to 6~8 by ammonia. After evaporating water on a hot plat, a gel formed. Then the gel was combusted on a furnace to remove organic compounds. The resultant green powders were calcined at 900°C for 5 h to yield homogenous oxides. The GDC and GSF powders were mixed with a weight ratio of 60:40, which is corresponding to a volume ratio of 55:45. After fully mixed, the resultant powder was pressed into disks under a pressure of ~200 MPa. Green disks were sintered at 1400°C for 3~5 h. GSF membranes used for comparison were sintered at 1250°C for 3 h. The relative density of all the composite membrane samples in this work was no less than 97%.

After polished to 0.5 mm, membranes were coated with $La_{0.6}Sr_{0.4}CoO_{3-\delta}$ (LSC) porous layer on air side to improve the oxygen surface exchange rate. A slurry of terpineol saturated by methylcellulose (60 wt %) mixed with LSC powder (40 wt %) was used to coat the membranes. The thickness of the porous layers was 10~20 μm. The LiLaNiO/γ-Al_2O_3 catalyst for partial oxidation of methane to syngas was prepared via the impregnation method.

Membrane reactor configurations and operation

Gold ring was used as sealant and sealed at 1000°C for long-term operation and POM reaction. Silver rings were used to seal GSF membrane and composite membrane of 1.0 mm in thickness at 960°C only for permeation tests. Oxygen permeation experiments were performed in a vertical high-temperature gas permeation cell. The effective inner-surface areas of the membrane discs were controlled around 0.85 cm^2. Operation temperatures were controlled by a microprocessor temperature controller (Model Al-708, Xiamen Yuguang Electronics Technology Research Institute, China) within ±1 K of the set points through a type-K thermocouple. Dried air was used as the feed gas and high purity helium was used as sweeping gas on the other side of the membrane. High purity CH_4 (or diluted by He) flowed on the reaction side of the membrane. Flow rates of all gases were controlled with mass flow controllers (Models D07-7A/ZM, Beijing Jianzhong Machine Factory, China). The effluents were analyzed by a gas chromatograph (GC, Agilent 6890) equipped with 13 X and Porapak Q columns. Oxygen permeation fluxes through membranes were calculated based on the effluent flow rate and the concentration of oxygen-containing compounds in the effluents. The calculation of oxygen permeation fluxes, selectivity, and conversion of POM reaction were based on the following five equations:

$$J_{O_2} = \frac{F_{CO} + 2F_{CO_2} + F_{H_2O} + 2F_{O_2(\text{unreacted})}}{2A} \quad (2)$$

$$F_{H_2O} = 2(F_{CH_4(\text{in})} - F_{CH_4(\text{out})}) - F_{H_2} \quad (3)$$

$$F_{H_2} = F_{\text{total}} - F_{CO} - F_{CO_2} - F_{CH_4(\text{out})} \quad (4)$$

$$X_{CH_4} = 1 - \frac{F_{CH_4}}{F_{CH_4} + F_{CO} + F_{CO_2}} \quad (5)$$

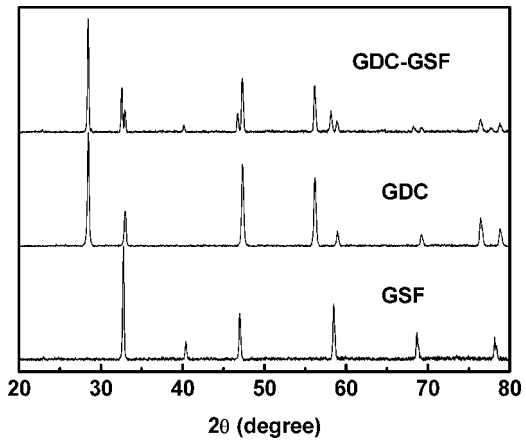

Figure 1. XRD patterns of GSF, GDC, and composite GDC-GSF.

The XRD pattern of the composite was obtained from a disk sintered at 1400°C for 3 h.

$$S_{CO} = \frac{F_{CO}}{F_{CO} + F_{CO_2}} \tag{6}$$

where F_i is flow rate of species i. X_{CH_4} and S_{CO} are conversion of CH_4 and selectivity of CO, respectively. A is the area of composite membranes. Leakage, due to the imperfect sealing, was calculated by Eq. 7.

$$\text{Leakage} = \frac{0.21}{0.79} \times \frac{C_{N_2}}{C_{O_2}} \times 100\% \tag{7}$$

where C_{O_2} and C_{N_2} are concentrations of oxygen gas and nitrogen gas detected by GC, respectively. Leakage is a ratio of oxygen leaking ($\frac{0.21}{0.79} \times C_{N_2}$) from feed side to the permeation side over total oxygen (C_{O_2}) in the permeation side. The leakages were less than 0.1% for both oxygen permeation and POM experiments, and had been subtracted when calculating oxygen permeation fluxes.

Characterization of membrane materials

Phase structure of membrane materials were determined by X-ray diffraction (XRD, Rigaku D/Max-RB, Cu Kα radiation) in a 2θ range of 20–80° with a step width of 0.02°. Lattice parameters were calculated by Rietveld method with an error of 0.0001 nm. Surface morphologies of membranes and local areas EDX analysis were observed on a Philips XL-30 scanning electron microscopy (SEM).

Results and Discussion

Phase development

Figure 1 shows the XRD patterns of GDC, GSF, and composite membrane GDC-GSF. As shown in the figure, new phases, such as $SrCeO_3$, $Gd_3Fe_5O_{12}$, cannot be detected. Both the lattice parameters of the fluorite phases (a = 0.5428 nm) and the perovskite phases (a = 0.3883 nm) are similar to GDC (a = 0.5427 nm) and GSF (a = 0.3861), respectively. These results suggest a good compatibility between the fluorite phase and perovskite phase, and reveal that Sr^{2+} possesses a lower chemical potential in the perovskite phase than in the fluorite phase for the GDC-GSF system. Kharton et al.[17,21] found that there was an expansion of the ceria lattice after composites sintered at high temperatures and attributed it to the incorporation of La^{3+} and Sr^{2+} into the ceria lattice. In this work, Gd^{3+} ion was used to replace La^{3+} to avoid the diffusing of La^{3+} ions into the ceria lattice. Considering the lower thermodynamic stability of Gd-contained perovskite oxides, the Gd doping amount is only 20% in the A-site. The similar lattice parameter of GDC in composite membrane and in pure state indicates that the chemical compatibility between the perovskite oxide and GDC can effectively be improved if Gd^{3+} is used as A-site ions.

Oxygen permeation performance

Figure 2 shows the oxygen permeation fluxes of mixed conductor of GSF at different temperatures. An oxygen permeation flux of 0.26 ml/(cm^2 min) is achieved at 940°C under an oxygen partial pressure gradient of 21 kPa/0.5 kPa for a 0.5 mm membrane. The result shows a mixed conducting of GSF. However, oxygen permeation flux of pure GDC is about 0.001 ml/(cm^2 min) determined by means of electrochemical cell.[17] It is because of its poor electronic conductivity in oxidizing atmosphere, although, the oxygen ionic conductivity is sufficient for permeation.

For dual phase composite oxygen permeable material, to keep the functions of the each phase, that is, one for oxygen ions transport and another for electron transport, the interdiffusion of metal ions between the two phases must be avoided or the interdiffusion has little influence on the performance of the membrane. Kharton et al.[17,21] reported that either the interdiffusion of metal ions between the two phases or the formation of new phases in the particle boundaries will decrease the oxygen ionic conductivity of the composite materials. Therefore, the interdiffusion leads to the degradation of the oxygen permeation flux of the composite membrane with time.[17] Figure 3 shows the dependence of oxygen permeation fluxes over time at the initial stage. It is interesting to be noted that the oxygen flux increases quickly at the

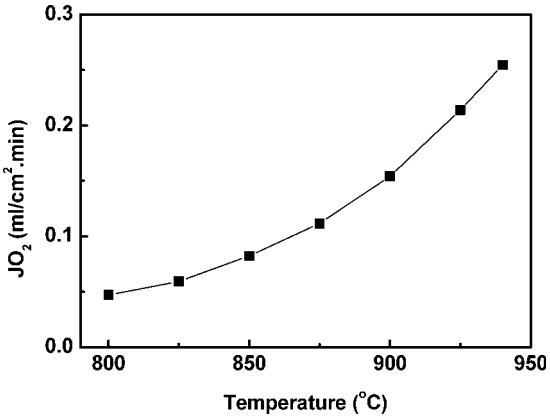

Figure 2. Oxygen permeation fluxes of GSF at different temperatures.

Air flow rate: 100 ml/min, 0.5 mm, oxygen partial pressure gradient: 21 kPa/0.5 kPa.

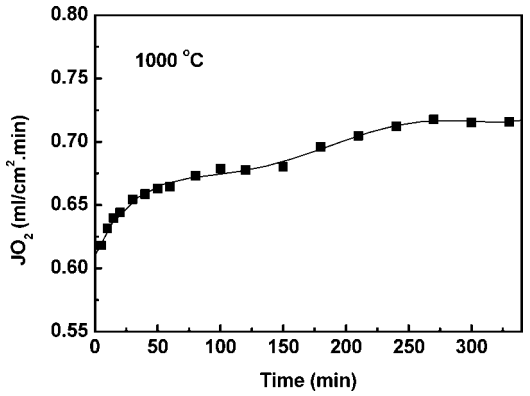

Figure 3. The dependence of oxygen permeation flux of GDC-GSF composite membrane on time at the initial stage at 1000°C.

He flow rate: 30 ml/min; air flow rate: 100 ml/min; membrane thickness: 0.5 mm. The solid line is only for visual guidance.

beginning, and then slowly 1 h later. It took about 600 h to reach the steady state. The oxygen flux increases from 0.46 to 0.63 ml/(cm^2 min), as shown in Figure 4. This phenomenon is hardly noticed in the perovskite oxygen permeable membrane. Usually, for single-phase perovskite membranes, oxygen permeation fluxes decrease with time at the initial stage and then reach a steady state. This unstable state in perovskite membranes is related to the readjusting of lattice structure from the as-prepared state to a steady state under permeation conditions or reduction of initial surface oxygen desorption rates.[4] In the case of the GDC-GSF, the mechanism of the increase of oxygen permeation flux with time is not clear now and should be investigated in detail.

Figure 5 shows the relationship between temperature and oxygen permeation fluxes of GDC-GSF composite membrane at different oxygen partial pressure gradients. The data were obtained after oxygen permeation process achieving a steady state. With the increase of oxygen partial pressure gradient,

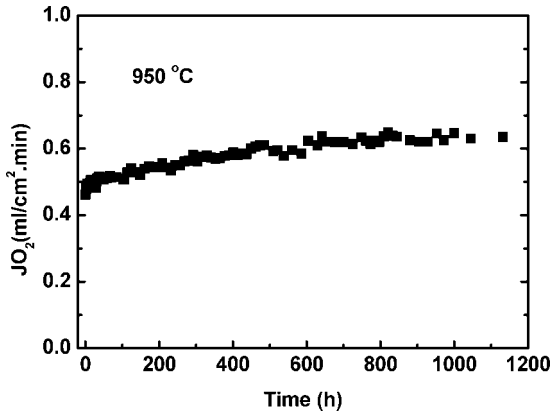

Figure 4. Long-term operation of oxygen permeation experiments of GDC-GSF composite membrane at 950°C.

He flow rate: 30 ml/min; air flow rate: 100 ml/min; membrane thickness: 0.5 mm.

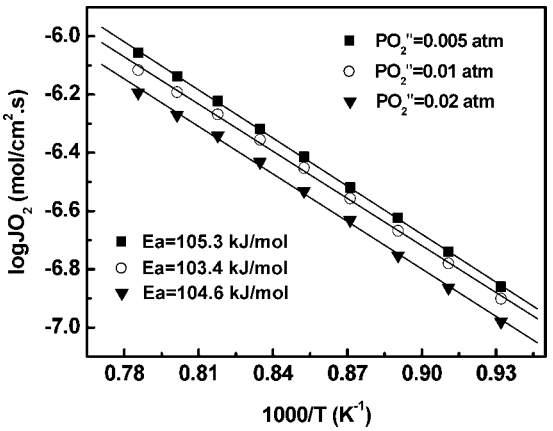

Figure 5. The relationship between temperature and oxygen permeation fluxes of GDC-GSF composite membrane at different oxygen partial gradients.

The oxygen partial pressures of the sweeping side were controlled by adjusting the He flow rate. Air flow rate: 100 ml/min; membrane thickness: 0.5 mm.

oxygen permeation fluxes enhance gradually, from 0.61 ml/(cm^2 min) at a gradient of 21 kPa/2 kPa to 0.80 ml/(cm^2 min) at a gradient of 21 kPa/0.5 kPa at 950°C. It can be found that the permeation fluxes of composite membranes are two times higher than that of GSF membrane and three orders higher than that of GDC under the similar conditions.[17] The high oxygen permeability of GDC-GSF composite membrane, compared with other ceria based composite membranes,[21,22] should be attributed to the mixed conducting property of GSF. Figure 5 also shows the activation energies (E_a) of oxygen permeation under different oxygen partial pressure gradients. The E_a values are similar, and close to that of GDC-LSM and GDC-LSCF composite membranes.[17,21] However, they are all larger than the oxygen ionic transport activation energy of GDC (73 kJ/mol),[21] which can be attributed to the occurrence of second phase and the limitation of oxygen surface exchange rate.

For composite membranes made of ionic conductors and pure electronic conductors, electronic conducting phase not only blocks the transport of oxygen ions, but also extends the way for transport of oxygen ions, as shown in Figure 6. Furthermore, partial ionic conducting phase or electronic conducting phase is totally enwrapped by another phase, which makes the enwrapped parts failed to conduct ions or electrons. Therefore, it is expected that ionic-electronic conducting composite membranes usually have poor permeability. Composite membranes like $Ce_{0.8}Gd_{0.2}O_{1.9}$-$La_{0.7}Sr_{0.3}MnO_3$ (GDC-LSM)[17], $Ce_{0.8}Sm_{0.2}O_{1.9}$-$La_{0.8}Sr_{0.2}CrO_3$ (SDC-LSCr),[22] and $Ce_{0.8}Gd_{0.2}O_{1.9}$-$La_{0.8}Sr_{0.2}Co_{0.2}Fe_{0.8}O_3$ (GDC-LSCF)[21] have been investigated in recent years. For the former two composite membranes, the electronic conducting phase of LSM or LSCr blocks the transport of oxygen ions from one fluorite grain to another. Although LSCF is a mixed conductor, the poor ionic conductivity (~0.01 S/cm at 950°C)[21] also blocks the transport of oxygen ions through the composite membrane. Therefore, these materials usually have poor permeability.

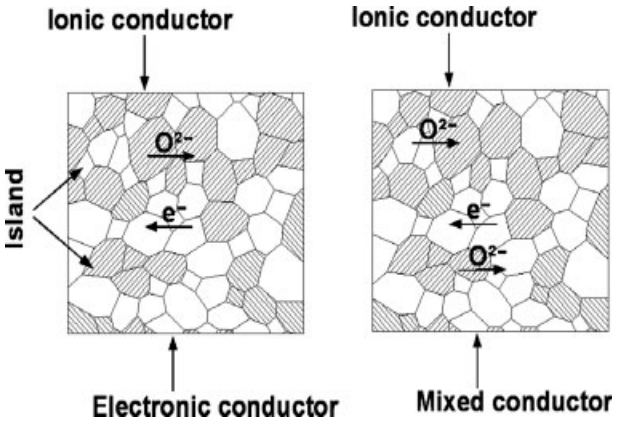

Figure 6. Schematic illustration of oxygen transport in ionic-electronic conductor composite membrane and ionic-mixed conductor composite membrane.

However, for composite membranes, like GDC-GSF, made of ionic conductors and mixed conductors, oxygen ions can transfer from ionic conducting phase to mixed conducting phase without increasing the tortuosity coefficient of the path, as shown in Figure 6. Every grains in those ionic-mixed conducting composite membranes help to oxygen permeation process.

The oxygen permeation fluxes of composite membranes regardless the block of electronic conducting phases can be calculated by the following two equations:

$$\sigma_{\text{ave}} = \sigma_{\text{F}} x_{\text{F}} + \sigma_{\text{P}}(1 - x_{\text{F}}) \tag{8}$$

$$J_{\text{O}_2,\text{cal}} = \frac{RT\sigma_{\text{ave}}}{16F^2L} \ln \frac{p'_{\text{O}_2}}{p''_{\text{O}_2}} \tag{9}$$

where x_{F} is volume fraction of fluorite phase in composite membranes; σ_{ave} is weighted average of oxygen ionic conductivity of fluorite and perovskite phase; σ_{F} and σ_{P} are oxygen ionic conductivity of fluorite and perovskite phase, respectively. p'_{O_2} and p''_{O_2} are high and low oxygen partial pressures of each side of the membrane, respectively. L is thickness of the membrane. $J_{\text{O}_2,\text{cal}}$ is oxygen permeation flux of the composite membrane regardless the block of electronic conducting phase. Other parameters have the usual meaning. The two equations are valid based on the suppositions of electronic conductivity in the mixed-conducting phase much larger than the ionic conductivity, and that the ionic conductivity is independent of oxygen partial pressure.

The difference between experimental oxygen permeation fluxes ($J_{\text{O}_2,\text{exp}}$) and calculated fluxes ($J_{\text{O}_2,\text{cal}}$) reveals the block degree of perovskite phase on the transport of oxygen ionic. Table 1 shows $J_{\text{O}_2,\text{exp}}$ and $J_{\text{O}_2,\text{cal}}$ values of several composite membranes. As shown in the table, the difference is small for composite membrane made of an ionic conductor and a mixed conductor, but large for composite membrane made of an ionic conductor and an electronic conductor. That is to say, mixed conducting perovskite phase has little block effect on oxygen transport process in composite membrane system compared with electronic conducting perovskite phase.

Figure 7 shows the influence of membranes thickness on the oxygen permeation fluxes. The dash line shows the oxygen permeation fluxes of the 1.0 mm membrane normalized to 0.5 mm. To do so, it was assumed that the oxygen permeation fluxes of the membranes are controlled by bulk diffusion and the influence of oxygen surface exchange can be ignored. As shown in the figure, there is a difference between the dash line (i.e., normalized values) and the values of the 0.5 mm membrane, which means that oxygen permeation is partially limited by oxygen surface exchange. Additionally, the difference becomes greater at lower temperatures, and the oxygen permeation activation energy of the 1.0 mm membrane (E_{a} = 94.5 kJ/mol) is smaller than that of 0.5 mm membrane (E_{a} = 105.3 kJ/mol). It can be concluded that the limitation of surface exchange becomes greater when reducing the thickness of composite membrane. Data shown in Figure 8 can make us further understand the surface exchange properties at different temperatures. According to the Wagner theory, if the oxygen permeation is controlled by bulk diffusion, the oxygen permeation flux will linearly increase with the oxygen partial pressure gradient. As shown in Figure 8, the oxygen fluxes linearly increase with the oxygen partial pressure gradient at 950°C, but nonlinearly at 850°C. Therefore, the oxygen flux across the membrane is mainly controlled by bulk diffusion at 950°C and partially limited by surface exchange at 850°C. Although the surface exposed to air was covered with LSC porous layer, the influence of surface exchange on oxygen flux was incompletely eliminated. One reason is the porous layer was partially sintered (shown in the following SEM pictures) and not the entire membrane surface was covered with the porous layer. Another reason is only the air side coated with LSC porous layer.

POM reaction and postoperation characterization

Partial oxidation of methane (POM) in the composite membrane has not been reported up to now. Therefore, the POM reaction was investigated to know the particular performance of the composite membrane.

Before conducting the POM reaction, the blank membrane catalytic oxidation of methane was investigated. Results showed the membrane had poor catalytic activity (methane conversion <3%) and C_2 selectivity (<45%) at 950°C.

Table 1. $J_{\text{O}_2,\text{exp}}$ and $J_{\text{O}_2,\text{cal}}$ Values of Several Composite Membranes at 950°C

Composite Membranes	Conditions		$J_{\text{O}_2,\text{exp}}$ [ml/(cm^2 min)]	$J_{\text{O}_2,\text{cal}}$ [ml/(cm^2 min)]	$J_{\text{O}_2,\text{exp}}/J_{\text{O}_2,\text{cal}}$	Ref.
	$\ln p'_{\text{O}_2}/p''_{\text{O}_2}$	Thickness (mm)				
GDC-LSM	1.84	0.6	0.074	0.282	0.262	17
GDC-LSCF	1.84	1.0	0.067	0.169	0.396	21
SDC-LSCr	3.13	0.3	0.188	1.233	0.152	22
GDC-GSF	3.74	0.5	0.804	0.871	0.923	This work

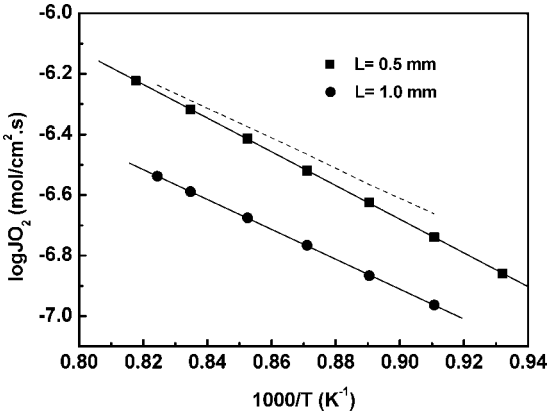

Figure 7. The influence of membranes thickness of GDC-GSF composite membrane on the oxygen permeation fluxes.

The dash line shows the oxygen permeation fluxes of the 1.0 mm membrane normalized to 0.5 mm. The oxygen fluxes were obtained under a constant oxygen partial gradient of 21 kPa/0.5 kPa. The oxygen partial pressures of the sweeping side were controlled by adjusting the He flow rate. Air flow rate: 100 ml/min.

POM reaction was carried out in a planar membrane reactor packed with unreduced 300 mg LiLaNiO/γ-Al_2O_3 catalyst. CH_4 (5 ml/min) diluted with He (20 ml/min) was introduced in the membrane reactor. After 30 min, the reaction reached a conversion of 30%, selectivity of ~100%, and oxygen permeation flux of 0.85 ml/(cm^2 min), as shown in Figure 9. After about 230 h operation, the conversion gradually increased to ~60%, and oxygen flux gradually increased to 2.4 ml/(cm^2 min). However, if we shut off the He supply and introduced the pure CH_4 into the membrane reactor, the conversion quickly increased to ~99%, and the oxygen flux immediately increased to 3.3 ml/(cm^2 min). Then after about 150 h operation at the conditions, the CH_4 flow rate gradually increased to ~10 ml/min. With the increase of CH_4 flow

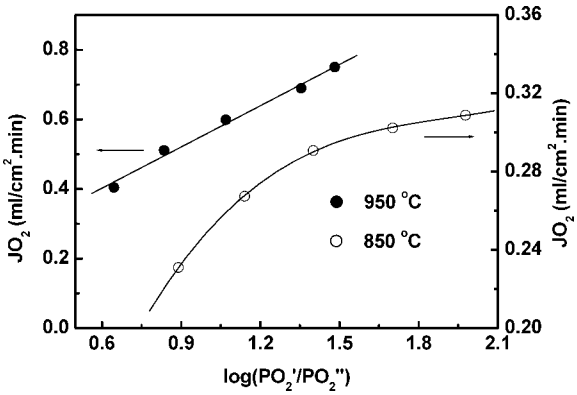

Figure 8. Dependence of the oxygen permeation fluxes through the composite membrane on oxygen partial pressure gradient at different temperatures.

The oxygen partial pressures of the sweeping side were controlled by adjusting the He flow rate. Air flow rate: 100 ml/min; membrane thickness: 0.5 mm. The solid lines are only for visual guidance.

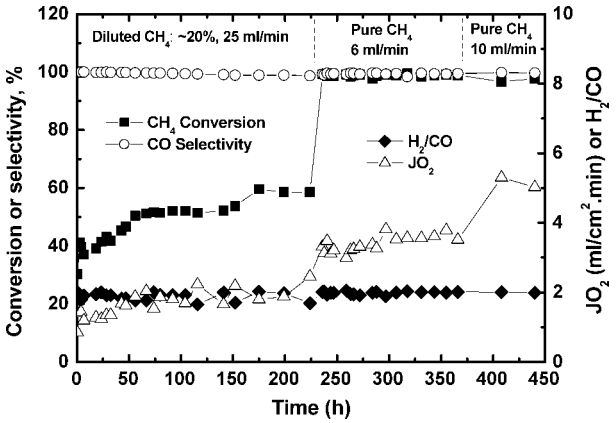

Figure 9. Long-term operation of partial oxidation of methane in the ceria based composite membrane reactor at 950°C.

Membrane thickness: 0.5 mm; air flow rate: 150 ml/min; CH_4 and He flow rate: shown in the figure; catalyst: 300 mg, 40~60 mesh.

rate, the oxygen permeation flux increased gradually and reached 5.2 ml/(cm^2 min) while the conversion and selectivity were keep constant in the whole process. Unfortunately, after 70 h operation under the conditions, the leakage began to increase gradually and exceeded the tolerance of the experiment after another 18 h. Therefore, the experiment had to be stopped. After the setup was disconnected, we found the surfaces quartz tube became loose after ~1600 h operation at 950°C, which caused the failure of the experiment. Although the POM reaction only operated 440 h, considerable oxygen permeation fluxes were obtained.

After the experiments, the detail changes of the membrane were investigated. Figure 10 shows the XRD patterns of the as-prepared and the used membrane of the reaction side. There are some changes in the pattern of the reaction side. Perovskite peaks shift to lower angles, which is corresponding to the reduction and expansion of the iron ions in the lattice. Additionally, $SrCO_3$ phase was also detected, indicating a decomposition of the perovskite phase to some extent.

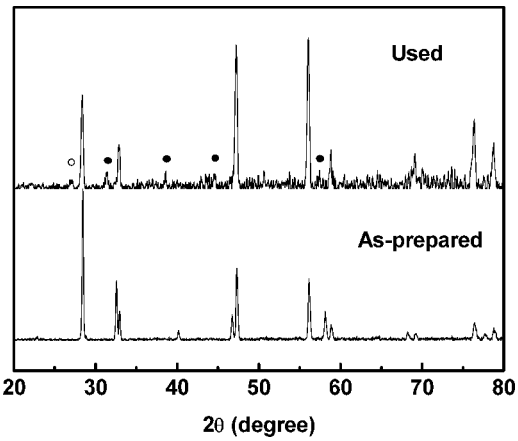

Figure 10. Comparison of the XRD patterns of the as-prepared and used membrane.

(●) Reduced perovskite oxide GSF; (○) $SrCO_3$.

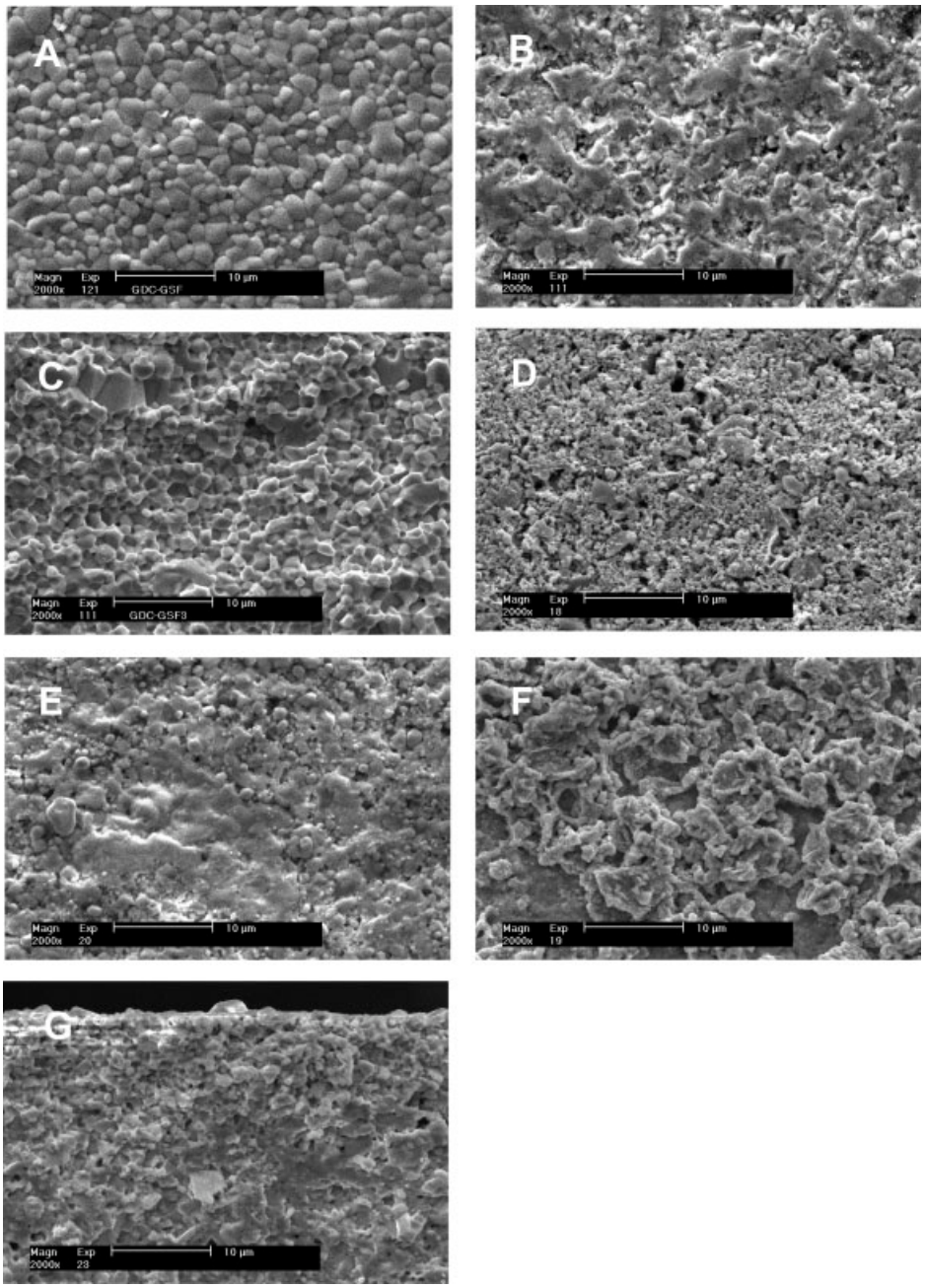

Figure 11. SEM pictures of the as-prepared and used membranes.

A,B (after polished), C,D (air side coated with LSC porous layer) of the as-prepared membrane; E (reaction side), F (air side), G of the used membrane; Top view: (A,B,D,E,F); cross-section: (C,G).

SEM and EDX analysis results showed in the Figure 11 and Table 2, respectively. Figure 11(A–D) showed the SEM pictures of the as-prepared membranes. As shown in Figure 11(A and C), the particles close pack together with a size of 1~3 μm. To obtain a relative density higher than 95%, the sintering temperature of GDC is usually up to 1600°C, but the occurrence of second phase of GSF can significantly decrease the sintering temperature. In this work, the composite membranes were sintered at 1400°C for 3~5 h, but the relative density of the membranes was higher than 97%. Compared with the polished membrane [shown in Figure 11(B)], the morphology of the used membrane of the reaction side [shown in Figure 11(E)] has no obvious changes. The cross section of the used membrane [Figure 11(G)] shows that the surface of the membrane can still keep dense after 1100 h oxygen permeation test and 440 h syngas production experiments. This reveals the good stability of the composite membrane. Figure 11(D and F) shows the top view of the air side of the fresh and used membranes, respectively. It was found that the porous LSC layer was partially sintered after 1600 h operation at 950°C, which resulted in the degradation of the catalytic activity to oxygen reduction.

Table 2. Local Areas EDX Results of the As-Prepared and Used Membranes

	O	Ce	Gd	Sr	Fe	Other	Sr/Fe
Fresh	62.7	14.0	5.5	7.9	9.9		0.80
Reaction side							
Surface	64.2	15.1	5.8	4.1	10.8		0.38
2 μm	67.2	12.8	5.2	7.1	7.7		0.92
10 μm	59.8	9.4	5.8	11.2	13.8		0.81
Middle	62.3	13.1	5.1	8.6	10.9		0.79
Air side							
5 μm	62.2	13.1	4.9	8.8	7.0	Co:3.2 La:0.8	0.86*

*Sr/(Fe + Co).

Table 2 shows the EDX results of the as-prepared and used membranes. As shown in the table, the ratio of Sr/Fe in middle section of the used membrane is similar to the as-prepared membrane. The transfer of metal elements only occurs at surface and a few microns depth of the composite membrane.

Conclusion

Composite oxygen permeable membranes comprise an oxygen ionic conducting fluorite oxide ($Ce_{0.8}Gd_{0.2}O_{1.9}$) for oxygen ions transport and a mixed conducting perovskite oxide ($Gd_{0.2}Sr_{0.8}FeO_{3-\delta}$) for both oxygen ions and electrons transport. XRD and 1100 h oxygen permeation test revealed that the fluorite phase and the perovskite were compatible with each other and can effectively form composite membrane for oxygen permeation. The oxygen flux reached 0.80 ml/(cm^2 min) at an oxygen partial pressure gradient of 21 kPa/0.5 kPa at 950°C. The composite membrane possesses high oxygen permeation flux because of the mixed conducting property of GSF. Under syngas production conditions, the oxygen flux increased to ~5.0 ml/(cm^2 min). After 440 h syngas production experiment, morphologies of the surface kept intact, but metal elements transfer up to several microns could not be avoided.

Acknowledgments

This work was supported financially by the Ministry of Science and Technology, China (Grant No. 2005CB221404), and National Science Foundation of China (50332040).

Literature Cited

1. Bouwmeester HJM, Burggraaf AJ. Dense ceramic membranes for oxygen separation. In: Gellings PJ, Bouwmeester HJM, editors. *The CRC Handbook of Solid State Electrochemistry*. Boca Raton: CRC, 1997:481–553.
2. Teraoka Y, Zhang HM, Furukawa S, Yamazoe N. Oxygen permeation though perovskite-type oxides. *Chem Lett*. 1985;1743–1746.
3. Teraoka Y, Nobunaga T, Yamazoe N. Effect of cation substitution on the oxygen semipermeability of perovskite-type oxides. *Chem Lett*. 1988;503–506.
4. Tsai CY, Dixon AG, Moser WR, Ma YH. Dense perovskite membrane reactors for the partial oxidation of methane to syngas. *AIChE J*. 1997;43:2741–2750.
5. Balachandran U, Dusek JT, Mieville RL, Poeppel RB, Kleefisch MS, Pei S, Kobylinski TP, Udovich CA, Bose AC. Dense ceramic membranes for partial oxidation of methane to syngas. *Appl Catal A*. 1995;133:19–29.
6. Shao ZP, Dong H, Xiong GX, Cong Y, Yang WS. Performance of a mixed-conducting ceramic membrane reactor with high oxygen permeability for methame conversion. *J Membr Sci*. 2001;183:181–192.
7. Dyer PN, Richards RE, Russek SL, Taylor DM. Ion transport membrane technology for oxygen separation and syngas production. *Solid State Ionics*. 2002;134:21–33.
8. Pei S, Kleegfisch MS, Udovich CA, Balachandran U. Failure mechanism of ceramic membrane reactors in partial oxidation of methane to syngas. *Catal Lett*. 1995;30:201–212.
9. Bouwmeester HJM. Dense ceramic membranes for methane conversion. *Catal Today*. 2003;82:141–150.
10. Kharton VV, Shaula AL, Snijkers FMM, Cooymans JFC, Luyten JJ, Yaremchenko AA, Valente AA, Tsipis EV, Frade JR, Marques FMB, Rocha J. Processing, stability and oxygen permeability of Sr(Fe, Al)O_3-based ceramic membranes. *J Membr Sci*. 2005;252:215–225.
11. Mackay R, Schwartz M, Sammels AF. Methods for separating oxygen from oxygen-containing gases. *US Patent*. 6,165,431. 2000.
12. Tong JH, Yang WS, Cai R, Zhu BC, Lin LW. Novel and ideal zirconium-based dense membrane reactors for partial oxidation of methane to syngas. *Catal Lett*. 2002;78:129–137.
13. Zhu XF, Wang HH, Yang WS. Novel cobalt-free oxygen permeable membrane. *Chem Commun*. 2004;1130–1131.
14. Lee TH, Yang YL, Jacobson AJ. Electrical conductivity and oxygen permeation of Ag/$BaBi_8O_{13}$ composites. *Solid State Ionics*. 2000;134:331–339.
15. Chen CS, Kruidhof H, Bouwmeester HJM. Thickness dependence of oxygen permeation through stabilized bismuth oxide-silver composite. *Solid State Ionics*. 1997;99:215–219.
16. Chen CS, Boukamp BA, Bouwmeester HJM, Cao GZ, Kruidhof H, Winnubst AJA, Burggraaf AJ. Microstructural development, electrical properties and oxygen permeation of zirconia-palladium composites. *Solid State Ionics*. 1995;76:23–28.
17. Kharton VV, Kovalevsky AV, Viskup AP, Yaremchenko AA, Naumovich EN, Marques FMB. Oxygen permeability of $Ce_{0.8}Gd_{0.2}O_{2-\delta}$-$La_{0.7}Sr_{0.3}MnO_{3-\delta}$ composite membranes. *J Electrochem Soc*. 2000; 147:2814–2821.
18. Shaula AL, Kharton VV, Marques FMB. Phase interaction and oxygen transport in $La_{0.8}Sr_{0.2}Fe_{0.8}Co_{0.2}O_3$–$(La_{0.9}Sr_{0.1})_{0.98}Ga_{0.8}Mg_{0.2}O_3$ composites. *J Eur Ceram Soc*. 2004;24:2631–2639.
19. Sirman JD, Chen JC. Ceramic membrane structure and oxygen separation method. *US Patent*. 6,514,314. 2003.
20. Nigge U, Wiemhöfer H-D, Römer EWJ, Bouwmeester HJM, Schulte TR. Composites of $Ce_{0.8}Gd_{0.2}O_{1.9}$ and $Gd_{0.7}Ca_{0.3}CoO_{3-\delta}$ as oxygen permeable membranes for exhaust gas sensors. *Solid State Ionics*. 2002;146:163–174.
21. Kharton VV, Kovalevsky AV, Viskup AP, Shaula AL, Figueiredo FM, Naumovich EN, Marques FMB. Oxygen transport in $Ce_{0.8}Gd_{0.2}O_{2-\delta}$-based composite membranes. *Solid State Ionics*. 2003;160:247–258.
22. Yi J, Zuo Y, Liu W, Winnubst L, Chen C. Oxygen permeation through a $Ce_{0.8}Sm_{0.2}O_{2-\delta}$–$La_{0.8}Sr_{0.2}CrO_{3-\delta}$ dual-phase composite membrane. *J Membr Sci*. 2006;280:849–855.

Manuscript received Jul. 2, 2007, revision received Sept. 24, 2007, and final revision received Nov. 29, 2007.